RSC Advances

ROYAL SOCIETY OF CHEMISTRY

www.rsc.org/advances

TOC Graphic

The unique network structure of V_2O_5 /f-MWCNT hybrid nanocomposite provides facile pathways for ion transport and enhances the electrochemical performance.

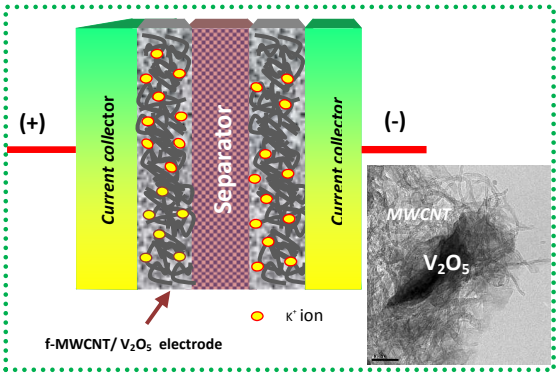

V_2O_5 / Functionalized MWCNT hybrid nanocomposite: the fabrication and its enhanced supercapacitive performance

Balakrishnan Saravanakumar [a], Kamatchi Kamaraj Purushothaman [b], Gopalan Muralidharan [c*]

ABSTRACT

The vanadium pentoxide (V_2O_5) has been attached to functionalized multiwall carbon nanotube (f-MWCNT) networks by simplified solution based approach. The product V_2O_5/ f-MWCNT hybrid nanocomposite has been exploited for supercapactior electrode application. The addition of f-MWCNT with V_2O_5 significantly improves the surface area and conductivity, which leads the high energy and power densities. This nanocomposite shows highest specific capacitance up to 410 Fg^{-1} and 280 Fg^{-1} at current densities of 0.5 and 10Ag^{-1} respectively. Moreover, this nanocomposite provides excellent energy density (~57 $Whkg^{-1}$), better rate capacity, and a good retention of capacity (~86%) up to 600 cycles of charge/discharge. Further A symmetric supercapacitor was fabricated using V_2O_5/ f-MWCNT nanocomposite as electrodes. It shows a specific capacitance of 64 Fg^{-1} at a current density of 0.5 Ag^{-1}.

KEYWORDS: f-MWCNT, *V_2O_5, aqueous electrolyte, network*

---

[a] Faculty of Physics, Mahalingam College of Engineering and Technology, Pollachi, Tamilnadu, India. Tel: +91 9843867704, Email: saravanakumar123@gmail.com

[b] Faculty of Physics, TRP Engineering College (SRM Group), Irungalur, Trichy, Tamilnadu, India. Tel: +91 90035 92066 Email: purushoth_gri@yahoo.co.in

[c*] Department of Physics, Gandhigram Rural Institute, Deemed university, Gandhigram, Tamilnadu, India. Tel: +91451 2452371, Fax: +91 451 2454466, E-mail: muraligru@gmail.com

Introduction

Energy requirements of 21st century compelled researchers to devote greater efforts at design and development of new advanced material architectures for energy storage applications. In the group of energy storage devices, supercapacitors captured enormous scientific interest because of its hallmark features like high power delivery, rapid charge discharge rate, and long utilizing life time.[1,2] Carbonaceous materials are employed as capacitor electrode and generally they store energy as charge accumulation at electrode/ electrolyte interface. Even though the carbon based electrodes provide high surface area and low resistivity, the energy density of the capacitor system is limited by the reduced double layer area which leads to smaller capacitance.[3] On other hand the transition metal oxides involve fast Faradic reactions and yield high value of specific capacitance values(> 1500 Fg^{-1}).[4]

The use of transition metal oxides and their performance for supercapacitors is hampered by two main issues, namely electrical conductivity and sluggish ion transport kinetics. Normally most of the pseudo capacitive materials show poor electrical conductivity and produces large electronic resistance when they act as electrodes. Blending of high conductivity material with pseudo capacitive metal oxides is expected to improve the conductivity of the electrode material. The problem of slow ion transport kinetics can be improved by fabrication of electrode materials with beneficial low dimensional architectures like nano structures.[5]

In this context, it is worth mentioning that functionalized carbon nanotube (MWCNT) has higher surface area (up to 475 $m^2 g^{-1}$), low resistivity and high stability.[6] Due to these useful features, MWCNT is used as a conductivity booster by many research groups.[7, 8] Among different pseudo capacitive materials vanadium pentoxide (V_2O_5) nanostructures have received

lot of attention as an electrode material for supercapacitors due to the multiple oxidation states exhibited by vanadium. Layered structure of this compound holds good interlayer sites for intercalation of another guest species.[9] Easy synthesis procedures of V_2O_5 facilitate preparation of V_2O_5 with different nano structures like nano flower[10], nano sheets[11] and nano fibers[12].

Design of innovative electrode materials helps improve the charge storage by both nonfaradic (capacitive) and Faradic nature and are of special interest as spotted in a few current publications. *Chen et al* [13] reported specific capacitance of 138 Fg^{-1} with an energy density of 18.8 $WhKg^{-1}$ for single-walled carbon nanotube/ RuO_2 nanowire. *Zhao et al.* fabricated Fe_2O_3/ MWCNT and achieved energy density of 50 $WhKg^{-1}$. [14] *Jin et al.* assembled graphene patched CNT/MnO_2 nanocomposite papers, which exhibit specific capacitance of 486.6 Fg^{-1} and an energy density of 24.8 $WhKg^{-1}$.[15] *Lei et al*. designed MnO_2 coated carbon nanotubes and showed specific capacitance of 193 Fg^{-1} with good cycling stability.[16] A hybrid of MnO_2 nanowires and MWCNTs demonstrated better rate capacity with an energy density of 17.8 $WhKg^{-1}$ reported by *Tang et al*.[17]

Inspired by these works, in the present study we employed a simple strategy to fabricate V_2O_5 with MWCNT for high performance supercapacitor electrode. The capping agent assisted co precipitation technique was adopted to synthesize V_2O_5/ f-MWCNT nanocomposite. The structural and electrochemical features of nano architectured V_2O_5/ f-MWCNT composite were investigated. The high electronic conductivity of MWCNT greatly improves the performance and exhibits high specific capacitance and superior energy density. Further, it reveals better capacity retention.

Results and discussion

Fig. 1 schematically represents the outline of the synthesis route of V_2O_5/ f-MWCNT nanocomposite. Initially the surfaces of MWCNTs are functionalized using concentrated acid mixture (3:1, H_2SO_4: HNO_3). It introduces carboxyl and hydroxyl functional groups on the surface of the MWCNT. This facilitates the dispersion of MWCNT and active centers for attachment with V_2O_5. The functionlization of MWCNT was confirmed by FTIR analysis as represented in Fig. S1 (ESI). Presence of bands at 1655, 1435 cm^{-1} in f-MWCNT spectra is attributed to keto –carbonyl and carboxyl functional groups. There is no such peaks were observed in unfunctionalized MWCNT.[18] This firmly indicates the attachment of functional groups with f-MWCNT. Further the stable f-MWCNT dispersion is blended with V_2O_5 solution make V_2O_5/ f-MWCNT nanocomposite. The morphological richness of V_2O_5/ f-MWCNT nanocomposite is characterized by scanning electron microscope (SEM) and transmission electron microscope (TEM). The SEM images of V_2O_5/ f-MWCNT nanocomposite as shown in Fig. 2 a, b. It confirms the presence of MWCNT networks in the nanocomposite. Further TEM images (Fig. 2 c, d, e) shows the f-MWCNT are strongly attached with the V_2O_5 and forms networks around the V_2O_5. The diameter of f-MWCNT (~9 nm) is also indicated in Fig. 2c. Here it is noted that the functionalization of MWCNT effectively enhances interaction between MWCNT and V_2O_5. The f-MWCNT network on V_2O_5 is expected to provide better electronic conductivity, unique structure and short diffusion pathways for electrolyte ion penetration. The weight percentage of elements present in the hybrid nanocomposite was confirmed through energy dispersive X-ray spectroscopy (EDS) analysis. The composite was prepared at room temperature and dried at 100^{o}C. So there is no possibility for decomposition/ evaporation of the

material. The EDS elemental mapping of V2O5/ f-MWCNT nanocomposite is presented in the Fig. 3. The three elements vanadium (69.03 wt%), oxygen (22.23 wt%) and carbon (8.73 wt%) in the mapping confirm the presence of MWCNT and V_2O_5 in the nanocomposite.

The X-ray diffraction patterns for the standard V_2O_5 and as-fabricated V_2O_5/ f-MWCNT nanocomposite material are presented in Fig 4a. It possesses diffraction peaks that belong to carbon is marked as "#" and V_2O_5 as "*". The V_2O_5 diffraction peaks are unambiguously indexed as orthorhombic structure (JCPDS Card No. 41−1426), Shcherbianite system with space group of Pmn (59) and cell parameters are a = 1.151 nm, b = 3.565 nm, and c = 4.372 nm. The diffraction peak at 26^0 corresponds to the MWCNT.[17] The existence of diffraction peaks of carbon and V_2O_5 confirms the attachment of V_2O_5 on highly conductive f-MWCNT network. The intimated inter connections of this V_2O_5/ f-MWCNT nanocomposite is expected to provide highly conductive channels for electrolyte penetration and better electrochemical performance.

Fig. 4b shows the nitrogen adsorption-desorption isotherm of V_2O_5/ f-MWCNT nanocomposite. The isotherm exhibits sharp capillary condensation step at high relative pressure and confirms the characteristic behaviour of type IV isotherm.[19] The presence of f-MWCNT in V_2O_5 shows improved specific surface area of 14.14 m^2/g compared to 7.1 m^2/g for V_2O_5 nanoporous network was reported in our previous work.[20] Addition of f-MWCNT with V_2O_5 nanoporous network provides 50% enhancement in specific surface area. It helps to achieve better electrochemical performance. The BJH model is used to determine the pore size distribution (PSD) profiles of the sample. The PSD profile reveals the presence of pores with diameter of 2, 8.5 nm in the sample and the total pore volume of 0.070146 cm^3/g. The pore size of 8.5 nm is attributed to the diameter of the MWCNT and 2nm is for the pores present in the

V_2O_5. This higher specific surface area and porous nature of V_2O_5/ f-MWCNT nanocomposite is expected to provide more active sites and it would be beneficial for charge storage.

The V_2O_5/ f-MWCNT nanocomposite is evaluated as a supercapacitor electrode material due to its appealing structural and morphological features. Fig. 5a shows cyclic voltammogram (CV) of the V_2O_5/ f-MWCNT nanocomposite. The nanocomposite electrode shows prominent anodic oxidation peak at 0.51 V and reduction at 0.4 V are typical peaks of the V_2O_5.[21] Further, two more not so prominent anodic (0.28 and 0.56V) and cathodic (0.23 and 0.41 V) peaks also could be identified. These peaks suggest a better expressive share of redox capacitance to the all inclusive capacitance. The specific capacitance of V_2O_5/ f-MWCNT nanocomposite electrode at a scan rate of 2 mVs^{-1} was derived to be 467 Fg^{-1}. This high value of capacitance is 48% higher than the pure V_2O_5 reported in our previous work.[20] Enhancement in specific capacitance is ascribed to the presence of f-MWCNT with V_2O_5. Fig. S2 (ESI) shows CV curves of MWCNT and functionalized MWCNT at a scan rate of 5 mVs^{-1}. The functionalized MWCNT electrode exhibits higher specific capacitance (53 Fg^{-1}) compared to MWCNT (20 Fg^{-1}). The f-MWCNT acts as a conductivity enhancer and also provides facile ion transport pathways through the electrode. These observations indicate that the union of highly conductive MWCNT and V_2O_5 plays a critical role by intensifying the specific capacitance of the electrode. The specific capacitance variation with different scan rats from 2 to 100 mVs^{-1} is presented in Fig. 5b, c. Increment in the scan rate reduces the specific capacitance continuously. It is due to inability of the ions to intercalate inner sites of the active materials in the electrode at higher scan rates.[22] The electrolyte ion does not have enough time to access the entire surface of the active material and results in broadening of redox peaks at higher scan rates. It is interesting to note that V_2O_5/ f-

MWCNT electrode shows 162 Fg^{-1} even at higher scan rate of 100mVs^{-1}. This kind of ability to withstand higher scan rates is quite beneficial in device applications.

To further explore its electrochemical goodness and quantify the discharge specific capacitance, the galvanostatic charge–discharge (GCD) analysis made for the V_2O_5/ f-MWCNT electrode at a current density of 0.5 Ag^{-1}. Fig. 5d shows the charge–discharge profiles of the V_2O_5/ f-MWCNT nanocomposite. The plot displays the small transition between the two linear portions of the profile. It indicates the overall capacitance is contributed from both EDLC and pseudoapacitance.[4] The calculated specific capacitance from GCD measurement is 410 Fg^{-1}. Fig. 5e shows the charge discharge profiles of V_2O_5/ f-MWCNT nanocomposite at different current densities ranges from 0.5 to 10 A g^{-1}. The variation of specific capacitance with current densities is shown in the Fig. 5f. It is noteworthy that the specific capacitance is still maintained as 280 Fg^{-1} at a fast charge/discharge rate of 10 A g^{-1} confirming the ability of the composite to withstand larger rates of intercalation and deintercalation of charges into it. Fig. 6a shows the cyclic stability of V_2O_5/ f-MWCNT nanocomposite electrode for 600 cycles at a current density of 10 Ag^{-1}. The retention of capacity decreased gradually with increasing the number of cycles. After 600 consecutive charge discharge cycles it retains 86% of initial capacity. For the pure V_2O_5 in our previous work we could obtain 76% retention. The formation of the composite has lead to 13% improvement in stability.

The Energy density (E, W hkg^{-1}) and power density (P, WKg^{-1}) are two important parameters for evaluating the performance of the supercapcitor electrodes. From GCD measurements the energy and power densities of f-MWCNT/ V_2O_5 electrodes are estimated. Fig. 6b gives the Ragone plot of the composite prepared in this work. The V_2O_5/ f-MWCNT electrode

possesses high energy density of 57 $Whkg^{-1}$ and power density of 250 WKg^{-1} at current density of 0.5 A g^{-1}. The energy density is remained as 38.8 $Whkg^{-1}$ when the power density increased to 5000 WKg^{-1} when the current rate was increased from 0.5A g^{-1} to 10 A g^{-1}. Recently *Shakir et al*. reported the energy density of 16 $Whkg^{-1}$ at 1 A g^{-1} for Ultra-thin vanadium oxide on multiwall carbon nanotubes. [23] *Chen et al*. presented the energy density of 40 $Whkg^{-1}$ for CNT/ V_2O_5 nanowire nanocomposite.[24] Compared to these reports V_2O_5/ f-MWCNT shows higher energy density value, which make this nanocomposite material as attractive for supercapacitor applications.

The best way to provide the realistic proof of better electrochemical performance of V_2O_5/ f-MWCNT is to look at the electrochemical impedance spectroscopy (EIS) measurements. They were carried out in the range of 0.01 Hz to 100 KHz. It provides the effect of charge transport, internal resistances and electrochemical kinetics on V_2O_5/ f-MWCNT nanocomposite. The resulting Nyquist impedance plot is shown in Fig. 6c. Fig. S3 (ESI) shows the equivalent circuit model to which the data was fitted. The symbols have their usual meaning as represented elsewhere.[20] The semicircle observed in the higher frequency range is related to the charge transfer resistance (R_{ct}) associated with the Faradaic reactions.[25] The observed charge transfer resistance of V_2O_5/ f-MWCNT nanocomposite is 0.98 Ω. This low value of charge transfer resistance indicates that the presence of a number of highly conductive ion migration channels for charge/ discharge process. Generally the perpendicular slope of the plot at low frequency region shows better capacitive behaviour.[26] Evidently, the slope of V_2O_5/ f-MWCNT nanocomposite is much steeper, indicating rapid electrolyte ion diffusion and enhancement in the capacitive performance. The frequency dependent specific capacitance plot of V_2O_5/ f-MWCNT nanocomposite is shown in Fig. 6d. The calculated maximum specific capacitance is 407 Fg^{-1} at

0.01 Hz. This value is in good agreement with the specific capacitance calculated from GCD method.

Finally, a symmetric supercapacitor was fabricated utilizing V_2O_5/ f-MWCNT as positive and negative electrodes and polypropylene separator to elucidate the performance of this nanocomposite electrode in a complete supercapacitor cell. A schematic of V_2O_5/ f-MWCNT based symmetric supercapacitor device is presented in the Fig. 7. The CV curves collected at different scan rates from 2-10 mVs^{-1} for V_2O_5/ f-MWCNT symmetric supercapacitor as shown in Fig 8a . The CV curves posses near rectangular shape and absence of sharp redox peaks. It is revealing the better capacitive behaviour of the device. The calculated specific capacitance of the device based on CV measurement are 81, 63, 43 Fg^{-1} at the scan rate of 2, 5, 10 mVs^{-1} respectively. The variation of specific capacitance with respect to scan rate is shown in Fig. 8b. The GCD curves with various current densities are shown in the Fig. 8c. The symmetrical GCD curves indicate the better reversibility and capacitive performance. The specific capacitance of 64, 41, 19 Fg^{-1} at the current densities of 0.5, 1, 2 Ag^{-1} were derived from GCD measurements. The specific capacitance variation with different current is shown in the Fig. 8d. The V_2O_5/ f-MWCNT based symmetric supercapacitor device exhibited energy density of 8.9 $Whkg^{-1}$ with the power density of 121 WKg^{-1}.

Conclusion

In summary, the V_2O_5/ f-MWCNT hybrid nanocomposite fabricated by a simple solution based low cost approach. The f-MWCNT acted as physical support for V_2O_5 and provides the unique morphology. It facilitates the effective pathways for ion penetration and enhances the

electrochemical performance of the V_2O_5. This hybrid nanocomposite has yielded 410 Fg^{-1} of specific capacitance which is nearly 50% more than those observed with pristine V_2O_5 prepared by us. The cyclic stability is improved by 13% while the R_{ct} value is reduced from nearly 5 Ω to 1 Ω which is one of the best things to happen when we need to perform fast charge discharge with super capacitor devices. Even at higher rates of charge discharge (10 Ag^{-1}) the capacity is quite large. These profitable features of V_2O_5/ f-MWCNT hybrid nanocomposite presented in the study are quite a promising electrode material for advanced supercapacitors.

EXPERIMENTAL METHODS

Materials and chemicals: The MWCNT (95 % Purity, 50 μm long) was purchased from Redex Nano technologies ltd India, Potassium permanganate [VII] and manganese [II] chloride was purchased from Merck India. Vanadium pentoxide, hydrogen peroxide (30%) and Potassium sulphate was obtained from SD fine Chemicals Ltd., India. Disodium citrate was purchased from Sigma Aldrich. All chemicals were of analytical grade and used directly without further purification.

Functionalization of MWCNT

The MWCNT were functionalized by anchoring carboxylic groups on the surface by chemical oxidation. The chemical oxidation of MWCNT was carried out with the help of 3:1 mixture of concentrated H_2SO_4/ HNO_3 solution. [27, 28] (The acid mixture is more corrosive in nature. Utmost care should be taken during handling.) About one gram of MWCNT is placed in a 500 ml round bottom flask. 75 ml of Conc. H_2SO_4 and 25 ml of Conc. HNO_3 is added with the MWCNT. The above mixture is transferred in to BOD incubator for constant agitation at 50°C for 12 hrs. Following this the suspension is permitted to cool down to atmospheric temperature.

Further the same quantity of DI water is added and filtered. The residue was washed with DI water several times until the pH reached to neutral (~7). The final products were dried at 100 ^{o}C for 5 hrs to get clean and dry functionalized MWCNT. The acid functionalized MWCNTs are denoted as f - MWCNTs.

Fabrication of V_2O_5/ f-MWCNT nanocomposite

In a typical synthesis, V_2O_5 (1.5959 g) was dispersed into 355 ml of double distilled water (DI). Slow dropping of 15 ml of 30% H_2O_2 solution to V_2O_5/ water mixture leads the vigorous bubbling. The color of the solution is changed from yellow to orange (Exothermic reaction). Subsequently the functionalized MWCNTs (0.1773g) were suspended into 20 ml of DI and prepared as suspension with the aid of an ultrasonicator (LOBA life, 42 kHz) for one hour. Then the suspension was added to V_2O_5 solution under vigorous magnetic stirring. Further disodium citrate (0.1773g) was added as controlling agent and the solution is stirred for 5 hrs to get the homogenous blend. The homogenous mixture was aged for 3 days at room temperature. The final products were collected by centrifugation and dried at 100 °C for 10 h in a hot air oven.

Characterization of F-MWCNT /V_2O_5 nanocomposite

The nanocomposite powders were characterized by X-ray diffraction (XRD) using a PANalytical X'pert- PRO diffractometer equipped with Cu Kα sealed tube (λ = 1.5406 Å). The sample was scanned in the range between 10 and 80° with a step size of 0.02° and exposure time of 10s. FTIR spectra were carried out using Perkin-Elmer Spectrum BX-II spectrophotometer using KBr pellets at room temperature. The nitrogen adsorption−desorption experiments were carried out by Micrometeritics ASAP 2020 analyzer. The Brunauer−Emmett−Teller (BET) method is used to calculate specific surface area. The porosity distribution of the samples were produced from desorption branch of the isotherm using the Barrett− Joyner−Halenda (BJH)

method. The SEM investigations were conducted on a JEOL JSM 3690 scanning electron microscope. TEM analyses were performed on a TEM-Philips JEOL CM12 microscope. Electrochemical characterizations like cyclic voltammetry (CV), galvanostatic charge−discharge, and electrochemical impedance spectroscopy (EIS) measurements were carried out using CHI 660 D electrochemical workstation (CH Instruments) at room temperature.

Electrode preparation and evolution

Electrochemical investigations of V_2O_5/ f-MWCNT nanocomposite samples were performed using a three-electrode cell set up, which consists of V_2O_5/ f-MWCNT as working electrode, platinum wire as counter electrode, and Ag/AgCl as the reference electrode. A mixture of the electrode material was prepared by combining 85 wt % sample, 10 wt % activated carbon (Sigma-Aldrich), and 5 wt % polytetrafluoroethylene (Sigma-Aldrich) with a few drops of ethanol. This slurry was pasted on to a Ultrasonically cleaned nickel foam (1 cm^2) surface. Then the material is dried at 80 °C for 8 hr to get the working electrode. The electrochemical tests were performed in 0.5 M K_2SO_4 aqueous electrolyte solution at atmospheric temperature. The symmetric supercapacitor setup was fabricated using V_2O_5/ f-MWCNT nanocomposite as positive and negative electrodes. The polypropylene (Celgard, 2400) is used as a separator. The specific capacitance and energy densities were derived based on the mass of the active material in the electrode.

The specific capacitance from CV observations can be derived by the following relation,

$$C = \frac{i}{v \times m}$$

Where C (Fg^{-1}) is the specific capacitance, m (mg cm^{-2}) is the mass of the active material, i (mA) is the average current and v (V) is the sweep rate.

The discharge specific capacitance from the discharge profiles by using the following relation

$$C_{dis} = \frac{I \times \Delta t}{m \times \Delta v}$$

Where I (ma), Δt (S), Δv (V) and m (mg cm^{-2}) are the current, discharge time, potential range and mass of the active material present in the electrode.

The specific capacitance values also calculated from the impedance measurements, using the following relation,

$$C_{imp} = \frac{1}{2\pi f Z''}$$

Where C_{imp} (Fg^{-1}), f (Hz) and Z*"*(Ohm) are specific capacitance from impedance data, frequency and impedance from imaginary part respectively.

The Energy density (E, $Whkg^{-1}$) and power density (P, WKg^{-1}) values are estimated based on the following relations,

$$E = \frac{1}{2} C(\Delta v)^2$$

$$P = \frac{E}{t}$$

Where C (Fg^{-1}), Δv (V), and t(s) are the discharge specific capacitance, potential window, and discharge time respectively.

Electronic Supplementary Information (ESI) available: FTIR and CV curves for MWCNT and f-MWCNT. The equivalent circuit model (Nyquist plot).

REFERENCES

1. P. Simon, Y. Gogotsi, *Nature materials*, 2008, 7, 845- 854.

2. X. Lang, A. Hirata, T. Fujita, M. Chen, *Nature Nanotechnology*, 2011, 6, 232- 236.

3. Z. Chen, Y. Qin, D. Weng, Q. Xiao, Y. Peng, X. Wang, H. Li, F. Wei, Y. F. Lu, *Adv. Funct. Mater.* 2009, 19, 3420- 3426.

4. Z. Lu, Z. Chang, J. Liu, X. Sun, *Nano Res*, 1, 4(7), 658- 665.

5. E. Frackowiaka, F. Beguin, *Carbon*, 2001, 39, 937- 950.

6. A. Manthiram, A. V. Murugan, A. Sarkar, T. Muraliganth, *Energy Environ. Sci*., 2008, 1, 621- 638.

7. X. Zhou, G. Wu, G. Gao, C. Cui, H. Yang, J. Zhen, B. Zhou, Z. Zhang, *Electrochimica Acta,* 2012, 74, 32-38.

8. X. Chen, H. Zhu, Y. C. Chen, Y. Shang, A. Cao, L. Hu, G. W. Rubloff , *ACS nano*, 2012, 6(9), 7948–7955.

9. Rui, X.; Lu, Z.; Yu, H.; Yang, D.; Hng, H. H.; Lim, T. M.; Yan, Q, *Nanoscale,* 2013, 5, 556–560.

10. Y. Tang, X. Rui, Y. Zhang, T. M. Lim, Z. Dong, H. H. Hng, X. Chen, Q. Yan, Z. Chen, *J. Mater. Chem. A*, 2013, 1, 82- 88.

11. X. Rui, Z. Lu, H. Yu, D. Yang, H. H. Hng, T. M. Lim, Q. Yan, *Nanoscale*, 2013, 5, 556-560.

12. D. Yu, C. Chen, S. Xie, Y. Liu, K. Park, X. Zhou, Q. Zhang, J. Li, G. Cao, Energy Environ. Sci., 2011, 4, 858- 861.

13. P. Chen, H. Chen, J. Qiu, C Zhou, *Nano Res,* 2010, 3, 594- 603.

14. X. Zhao, C. Johnston, P. S. Grant, *J. Mater. Chem*., 2009, 19, 8755- 8760.

15. Y. Jin, H. Chen, M. Chen, N. Liu, Q. Li, *ACS Appl. Mater. Interfaces*, 2013, 5, 3408- 3416.

16. Z. Lei, F. Shi, L. Lu. *ACS Appl. Mater. Interfaces*, 2012, 4, 1058- 1064.

17. W. Tang, Y. Y. Hou, X. J. Wang, Y. Bai, Y. S. Zhua, H. Sun, Y. B. Yue, Y. P Wu, K. K. Zhu, R. Holze, *Journal of Power Sources*, 2012, 197,330- 333.

18. H. J. Lee, S. W. Han, Y. D. Kwon, L. S. Tan, J. B. Baek, Carbon,2008, 46, 1850–1859.

19. S. I. Kim, J. S. Lee, H. J. Ahn, H. K. Song, J. H. Jang, *ACS Appl. Mater. Interfaces*, 2013, 5(5), 1596-1603.

20. B. Saravanakumar, K. K. Purushothaman, G. Muralidharan, *ACS Appl. Mater. Interfaces,* 2012, 4(9), 4484- 4490.

21. G. Wee,H. Z. Soh, Y. L. Cheah,S. G. Mhaisalkar, M. Srinivasan, *J. Mater. Chem*. 2010, 20, 6720- 6725.

22. S. Vijayakumar, A. K. Ponnalagi, S. Nagamuthu, G. Muralidharan, *Electrochimica Acta,* 2013,106, 500- 505.

23. I. Shakir, J. H. Choi, M. Shahid, S. A. S Shahid, U. A. Rana, M. Sarfraz, D. J. Kang, *Electrochimica Acta*, 2013, 111, 400- 404.

24. Z. Chen, V. Augustyn, J. Wen, Y. Zhang, M. Shen, B. Dunn, Y. F. Lu, *Adv. Mater.,* 2011, 23, 791- 795.

25. A. Yuan. Q. Zhang, *Electrochem. Commun.,* 2006, 8, 1173- 1178.

26. D. W. Wang, F. Li, H. T. Fang, M. Liu, Q. Lu, H. M. Cheng, *J. Phys. Chem. B*, 2006, 110, 8570- 8575.

27. V. Datsyuk, M. Kalyva, K. Papagelis, J. Parthenios, D. Tasis, A. Siokou, I. Kallitsis, C. Galiotis, *Carbon*,2008, 46, 833- 840.

28. G. Zhang, S. Sun, D. Yang, J. P. Dodelet, E. Sacher, *Carbon*, 2008, 46, 196- 205.

Figures and Captions

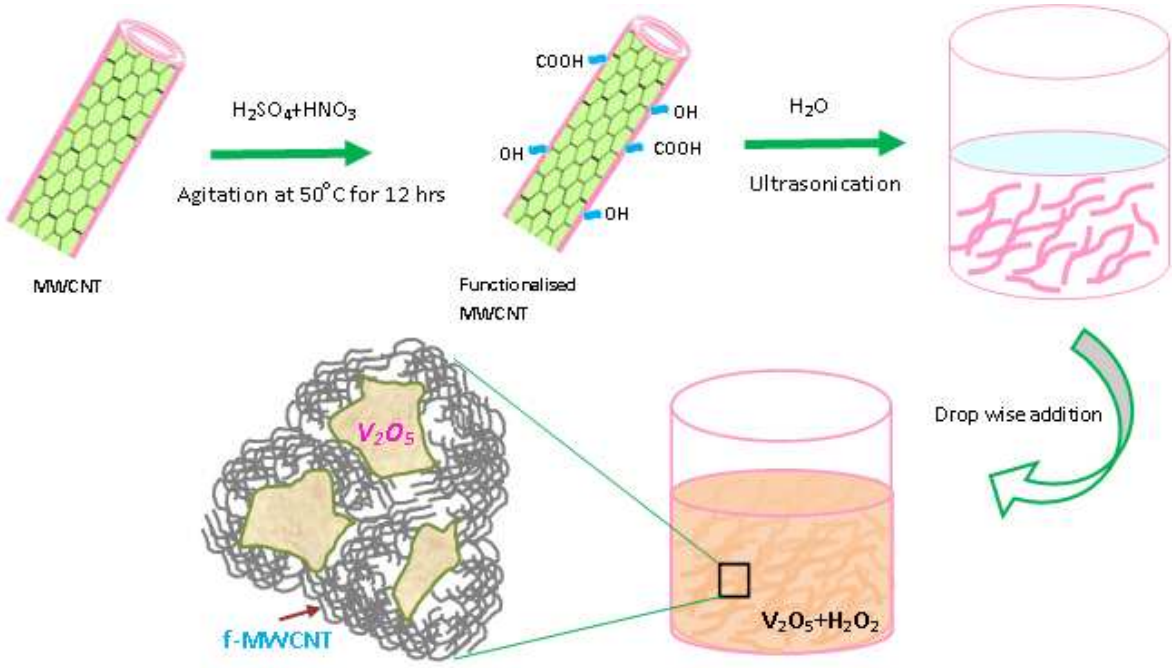

Fig 1. Schematic outline of the synthesis route to V_2O_5/ f-MWCNT nanocomposite

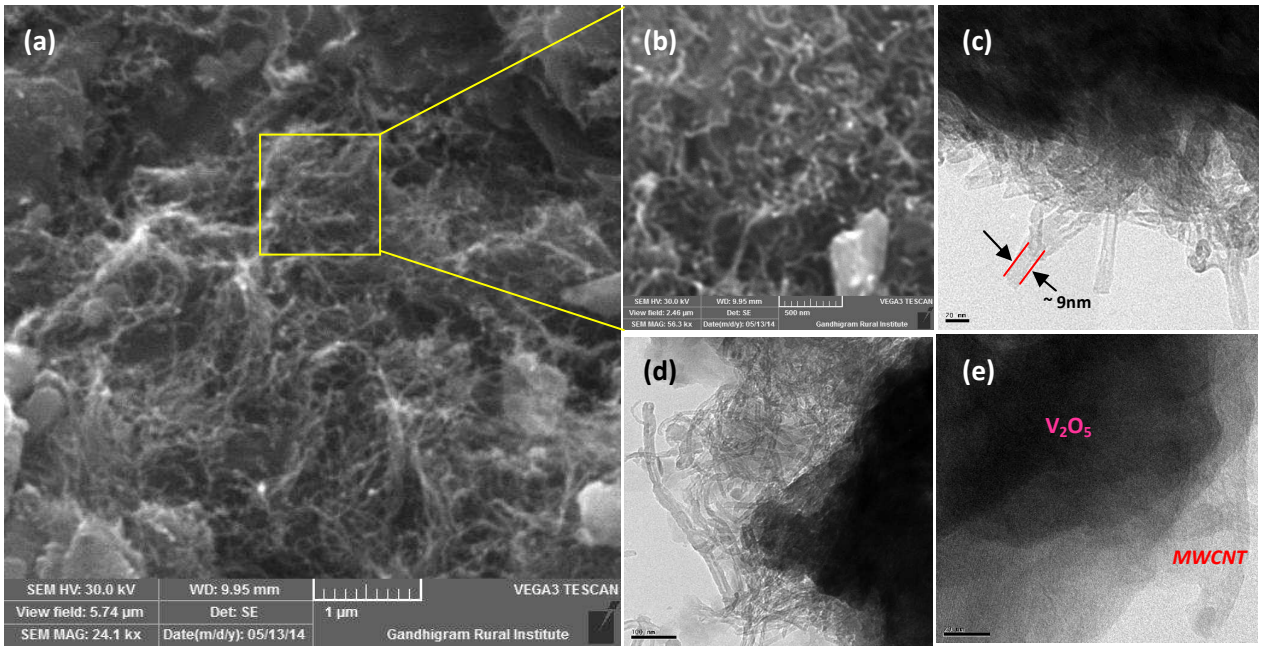

Fig 2. (a, b) SEM images of V_2O_5/ f-MWCNT. (c, d, e) TEM images of V_2O_5/ f-MWCNT at different magnifications.

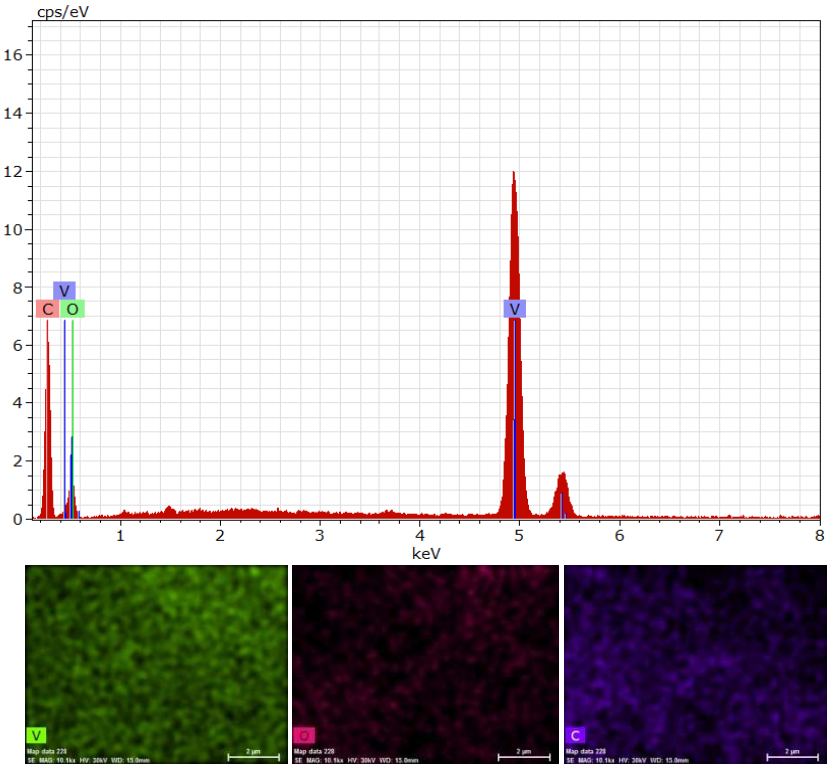

Fig 3. EDS Spectrum and elemental mapping of V_2O_5/ f-MWCNT hybrid nanocomposite

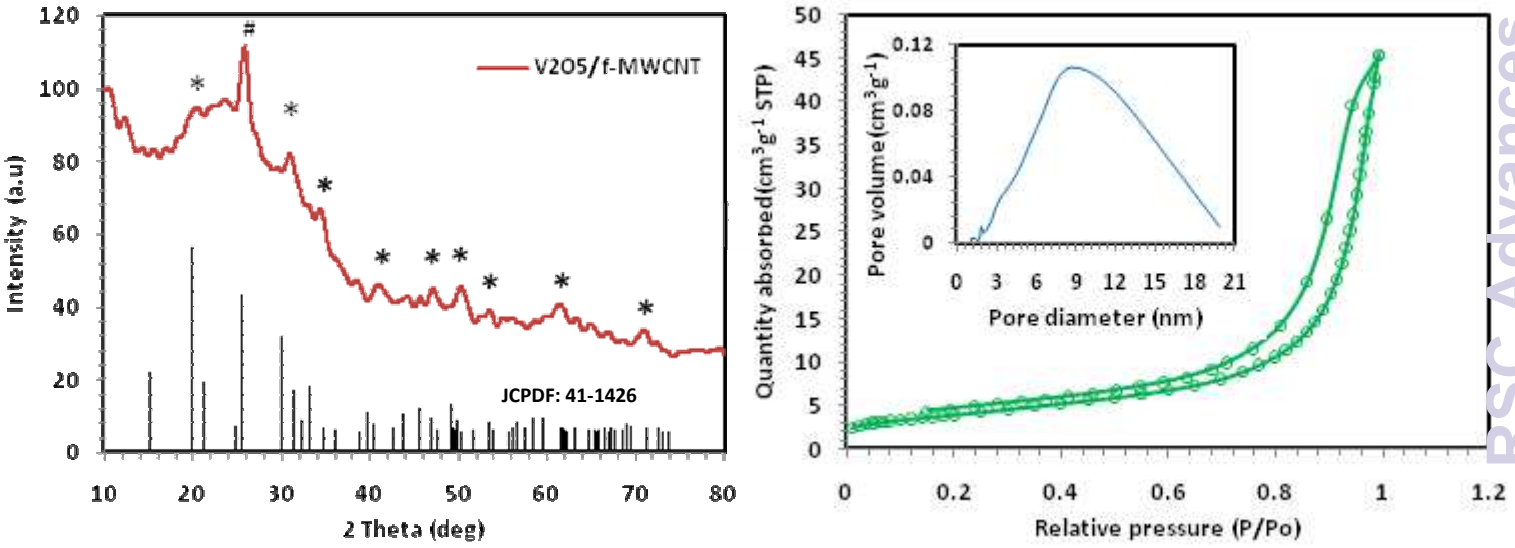

Fig 4. (a) XRD pattern of V_2O_5/ f-MWCNT nanocomposite. (b) Nitrogen adsorption/ desorption isotherms of V_2O_5/ f-MWCNT. Inset showing the pore size distribution curve.

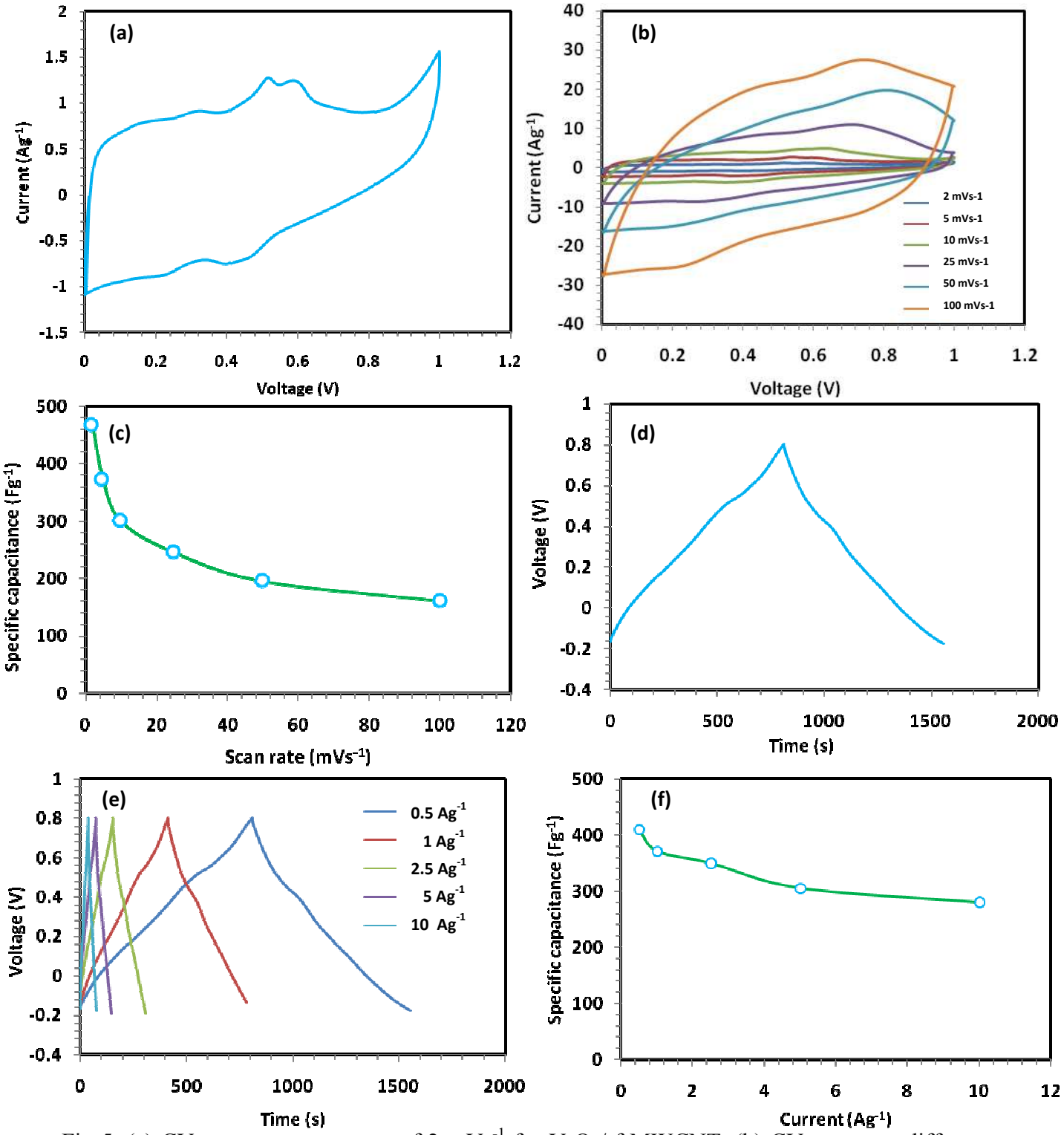

Fig 5. (a) CV curve at a scan rate of 2 mVs^{-1} for V_2O_5/ f-MWCNT. (b) CV curves at different sweep rates. (c) Specific capacitance as a function of scan rates. (d) Charge /discharge profile of V_2O_5/ f-MWCNT at $0.5Ag^{-1}$. (e) Charge /discharge profiles at different current densities. (f) Variation of specific capacitance as a function of current density.

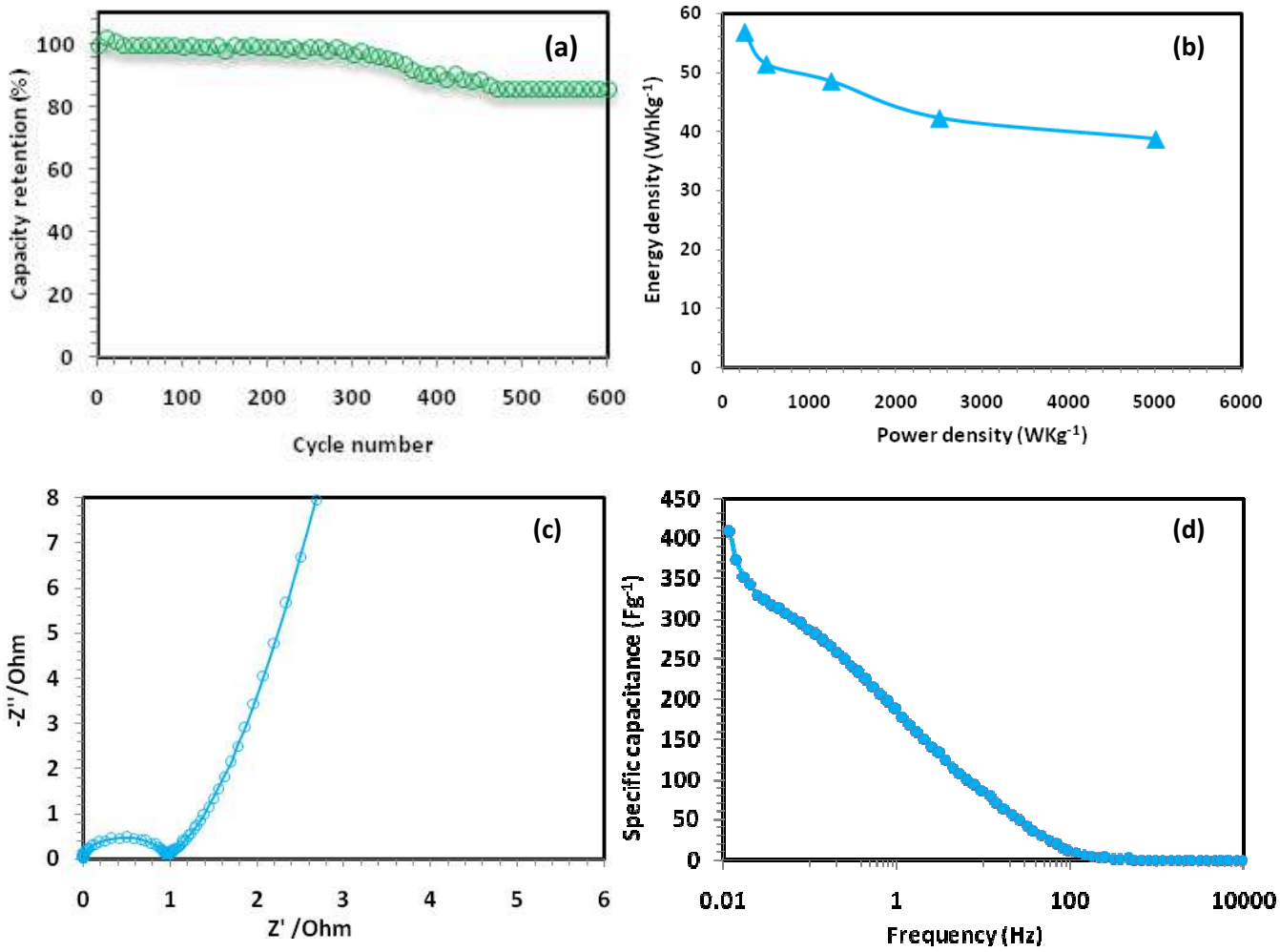

Fig 6. (a) Charge/ discharge cyclic test of V_2O_5/ f-MWCNT electrodes at a current density of 10 Ag^{-1}. (b) Ragone plot for V_2O_5/ f-MWCNT. (c) Nyquist plot of V_2O_5/ f-MWCNT. (d) Specific capacitance variation as a function of frequency, derived from impedance measurements

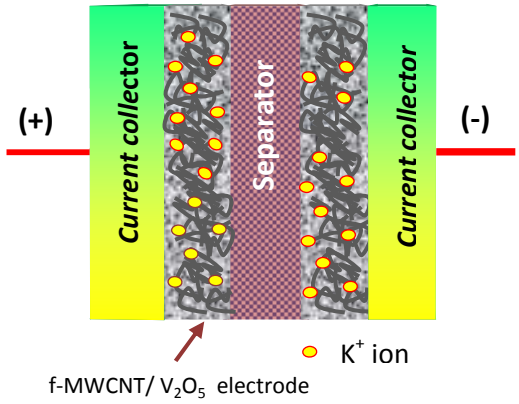

Fig 7. Schematic of V_2O_5/ f-MWCNT based symmetric supercapacitor device.

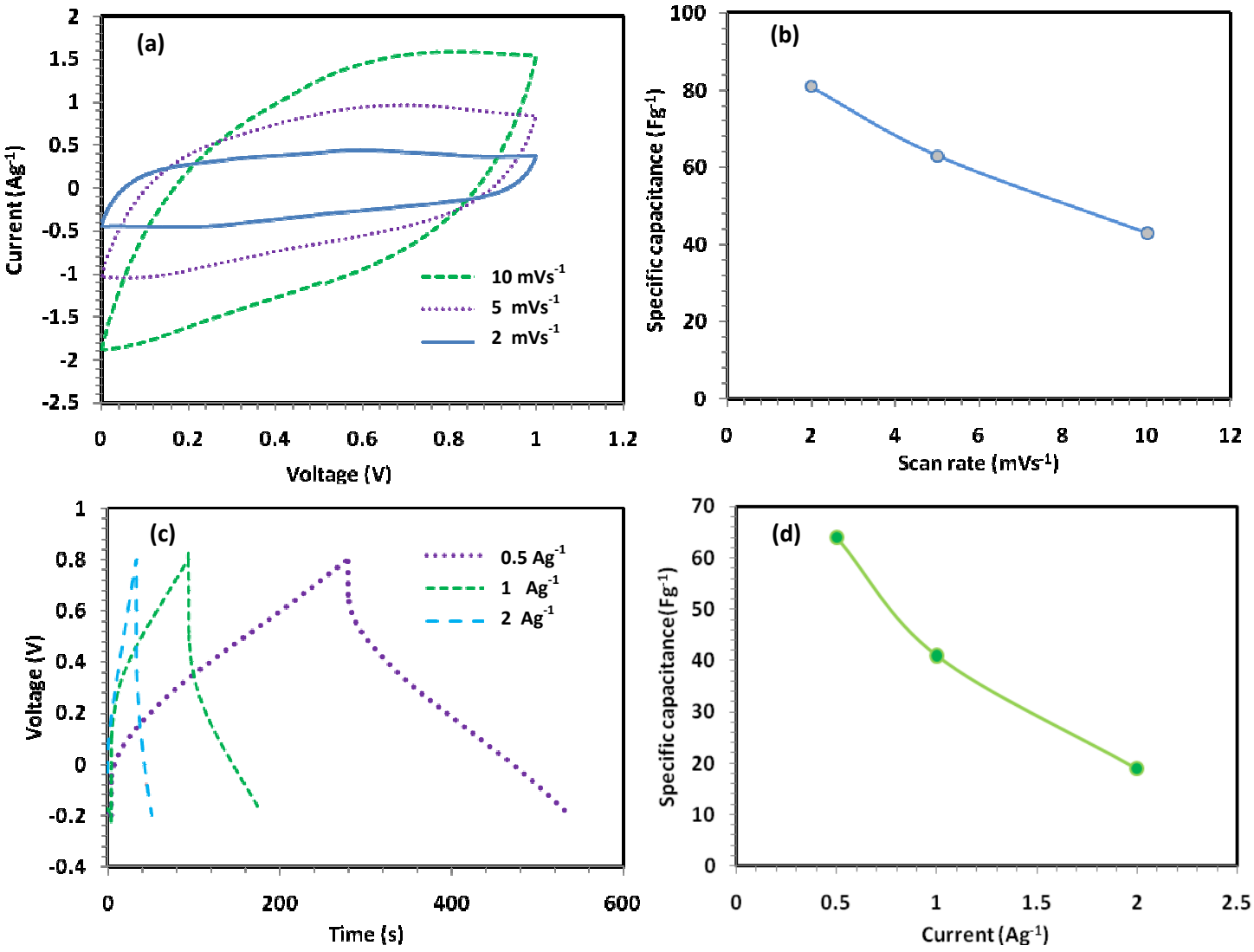

Fig 8. (a) CV curves of V_2O_5/ f-MWCNT symmetric supercapacitor at scan rate from 2 to 10 mVs^{-1} (b) Specific capacitance variation with the scan rate (c) Charge/ discharge curves of f-MWCNT/ V_2O_5 symmetric supercapacitor at the current density of 0.5 to 2 Ag^{-1}. (d) Specific capacitance variation with the current density.